Research Square

Preprints are preliminary reports that have not undergone peer review.
They should not be considered conclusive, used to inform clinical practice,
or referenced by the media as validated information.

Synthesis of Gelatin-Cellulose Nanocrystals Hydrogel Membrane For Removal of Cu (II) And Co (II) From Mining Processes Wastewater

John Kabuba (johnka@vut.ac.za)
Vaal University of Technology Faculty of Engineering and Technology
Trésor Lukusa
Vaal University of Technology Faculty of Engineering and Technology

Research Article

Keywords: Gelatin, Cellulose, nanocrystals, Copper (II) and Cobalt (II) removal, Adsorption, Hydrogel membrane

Posted Date: May 28th, 2021

DOI: https://doi.org/10.21203/rs.3.rs-383692/v1

License: This work is licensed under a Creative Commons Attribution 4.0 International License.
Read Full License

Synthesis of Gelatin-cellulose nanocrystals Hydrogel Membrane for removal of Cu (II) and Co (II) from mining processes wastewater

John Kabuba* and Trésor Lukusa

Department of Chemical Engineering, Faculty of Engineering and Technology, Vaal University of Technology, Vanderbijlpark, Private Bag X021, South Africa

*Tel.: +27 16 950 9887, Fax: +27 16 950 9687, *E-mail: johnka@vut.ac.za*

Abstract

This study describes the removal of Cu (II) and Co (II) ions from mining processes wastewater using synthesis of Gelatin-cellulose nanocrystals (CNCs) hydrogel membrane (GCHM). In a batch experiment, the influence of different parameters such as pH, contact time, temperature, and ratio of gelatin and CNCs was evaluated. Higher removal efficiency was obtained at ratio 3÷1 and at pH 5 and 7 for Cu (II) and Co (II), respectively, and a contact time of 120 mins and a temperature of 30°C. The experimental data fitted satisfactory to Freundlich isotherm model. The adsorption of metal ions has been fit by the particle diffusion model. The results revealed that gelatin and CNCs were identified as the low-cost and promising adsorption material for the removal of heavy metals from wastewater.

KEYWORDS: Gelatin, Cellulose, nanocrystals, Copper (II) and Cobalt (II) removal, Adsorption, Hydrogel membrane.

Introduction

Heavy metals such as copper, cobalt, zinc, nickel, cadmium, and lead in wastewater from mining process are toxic, not biodegradable and pose several health problems even at low concentrations (Abdulrahman Oyekamni et al., 2019). Therefore, the removal of these heavy metals from wastewater is mandatory prior to its release into the environment. Conventional removal methods such as coagulation, flotation, solvent extraction, ion-exchange, reverse osmosis, bioremediation, electrodialysis and adsorption have been developed to remove copper and cobalt ions from wastewater (Abdulkareem et al., 2013; Garcia-Diaz et al., 2018; Kabuba, 2019; Kabuba et al., 2019). Adsorption is the most frequently used removal methods due to its low operating cost and possible regeneration of adsorbents (Garcia-Diaz et al., 2018). Different

types of adsorption materials have been developed. Cellulose nanocrystals (CNCs) and gelatin were found to be the most materials used in adsorption methods (Akpomie et al., 2015; Silva Filho et al., 2013). Gelatin is low-cost protein, commercially available, biodegradable, film-forming properties, transparency and presenting good processibility obtained by the partial hydrolysis of collagen at controlled pH and temperature conditions (Joshi, Rawat & Bohidar, 2018). CNCs are one of the most studied polysaccharide-based nanomaterials in polymer nanocomposites, biodegradable, and non-toxic characteristics (Noorbakhsh-Soltani, Zerafat & Sabbaghi, 2018; Moon et al., 2011). CNCs were synthesized and incorporated in gelatin to increase the surface area which is required to improve the efficiency in the interaction with heavy metals ions (Oyewo et al., 2019; Leite et al., 2020). Hydrogel containing CNCs have good biocompatibility and biodegradability, can be used in water treatment as filtration membrane where the solution goes through the hydrogel membrane film as described for gel membrane permeation (Ahmed, 2015; Fujiyabu et al., 2017; Getachew et al., 2017; Marks et al., 2019; Tran et al., 2018; Yao et al., 2019). Due to the abundance of ion-coordinating sites and their aptitude to adsorb a large amount of water, hydrogel films have recently founded another application in water treatment to remove heavy metal ions using adsorption method (Alizadehgiashi et al., 2018; El-Halah and Lopez-Carrasquero, 2018; Perumal et al., 2019; Qi et al., 2019; Zhang et al., 2019). Literature review revealed that no work, in which efficiency of Gelatin-cellulose nanocrystals hydrogel membrane (GCHM) for the heavy metal ions removal from aqueous solution has been investigated. Therefore, the objective of this study was to determine the effects of various experimental variables for the removal of Cu (II) and Cu (II) onto GCHM.

Materials and methods

Adsorbate, adsorbent preparation and sampling procedure

Wastewater samples were collected from mining plant effluent in Rustenburg, South Africa. The samples were placed in 1000 mL plastic bottles, hold in cooler boxes and stored overnight in the fridge prior to the experiments. The characteristics of the wastewater used in the experiments is presented in Table 1.

All chemicals and reagents used in the work were analytical reagent grade purchased from Sigma-Aldrich, South Africa. Adequate quantities of CNCs and gelatin (purity ≥ 98%) were supplied by CSIR and dispersed in 50 mL of water. The CNCs suspension was then homogenized using a homogenizer to ensure the CNCs suspended uniformly. Certain amount of gelatin was then added into CNCs suspension. The mixture was then stirred at 55°C until a

homogeneous viscous mixture was obtained. Table 2 presented the ratios composition of GCHM hydrogel.

The cross-linking agent (EDTA 1%) was then added drop wise. After 4 hours, the mixture was poured into a petri dish and placed in oven at 45°C until the mixture was dried. Hydrogels as films were removed from the petri dish and washed with distilled water to remove unreacted chemicals. The unreacted chemicals have been removed from hydrogel using acetone (Yao, 2019; Yin and Amin, 2014).

Batch adsorption experiment

The adsorption of Cu (II) and Co (II) ions by GCHM was tested in batch experiment. A shaker was used for mixing the solution. Several operational parameters were optimized, and this includes effects of pH, gelatin-CNCs ratios, contact time and temperature. To ensure validity of the results and reputability, all experiments were performed in triplicate and the data were reported as an average value at 95% confidence level ($p > 0.05$). Heavy metal ions uptake capacity and the removal efficiency were calculated using Equations 1 and 2, respectively.

$$qe = \frac{Co-Ce}{m} \times V \quad (1)$$

$$\%\, removal = \frac{Co-Ce}{Co} \times 100 \quad (2)$$

where qe (mg/g): amount of metal ions adsorbed per unit mass of adsorbent, Co (mg/L): initial concentration of metal ions, Ce (mg/L): amount of metal ions at equilibrium, V (L): volume of solution used and m (g): mass of the adsorbent.

The experiments were carried out in 250 mL of plastic container, at a constant agitation speed (250 rpm) with 100 mL solution. Amount of 0.25 g of GCHM was added into 100 mL of binary metal ions solution and the mixtures were placed in a rotary shaker between 15 and 120 min. The effect of temperatures ranging between 30°C and 75°C was investigated using thermo-shaker. The solution of binary metal ions was adjusted in pH solutions between 3 and 7 using 1M of HCl and NaOH solutions.

Results and discussion

Characterization of Hydrogel

The samples of cellulose, gelatin and their mixtures have been prepared on the disc of CaF_2 and analysed to Midac FTIR 5000 Spectrophotometer. The absorption FTIR spectra obtained are shown in Figures 1-4.

The CNCs has shown the characteristic bands around 3000 and 3650 cm^{-1} that represents the strong elongation vibration band of the OH function. At 2950 cm^{-1}, it is observed an elongation

vibration band for bound C-H that is confirmed by the deformation band around 1500 cm^{-1}. The band around 1450 cm^{-1} is the vibration shear of CH_2 (Alemdar and Sain, 2008; Sain and Panthapulakkal, 2006). The peak at 1700 cm^{-1} is characteristic of the elongation vibration band of the carboxyl (C=O) confirmed by the characteristic band around 890 cm^{-1} that corresponds to the C-H of aldehyde group (Münster et al., 2017). The peak around 1000 cm^{-1} is attributed to OH function (Tran et al., 2018). The FTIR spectra of gelatin have present the characteristic peaks around of 2955 cm^{-1} for the vibration band of the amide A, of 2700 cm^{-1} for the vibration band of the amide B, of 1600 cm^{-1} for the vibration band of the amide (I), of 1500 cm^{-1} for the vibration band of the amide (I), of 1500 cm^{-1} for the vibration band of the amide (II) and of 1200 cm^{-1} for the vibration band of the amide (III). The amide (III) is represented by the combination of the elongation vibration peaks of C-N and the deformation vibration peaks of N-H. Moreover, the amide (I) is characterized by the elongation vibration of C=O to which is added a contribute band of elongation vibration of C-N, of deformation out-of-plan of C-C-N. Finally, the amide (II) is characterized by the elongation vibration band of C-N and that of out-of-plane deformation of N-H out-of-plan (Merina et al., 2017; Fernandes de Almeida et al., 2012; Silvestein et al., 2007). The peaks below 1000 cm^{-1} are characteristic of low molecular weight amides (Silvestein et al., 2007).

After analyzing the FTIR spectra of gelatin and CNCs, the spectra of the mixtures of gelatin and CNC in proportions A, B, and C were analyzed (Fig. 3).

A comparison of the values of different bands shows a bathochromic effect coupled with a decrease in the intensity of certain bands (Feinsten, 1995). The bands are appearing between 2400 and 3600 cm^{-1} (N-H and O-H) for mix A which moves to 3000 and 3600 cm^{-1} for mix B up to 3240-3634 cm^{-1} for the mix C. The same phenomenon is observed with the C=N band which moves from 1490 cm^{-1}, at 1550 cm^{-1} to 1650 cm^{-1} when moving from ratio A, B, and C, respectively for the gelatin-cellulose mixture. In addition, they were observed a slight constancy of the carboxyl band at 1700 cm^{-1} except for the intensity of the band which increased slightly when going from ratio A to B.

The bathochromic effect observed with increasing gelatin content is evidence that new bonds are created and therefore new functions are created. Therefore, it observes the disappearance of certain bands and the decrease in the intensity of others. The optimum ratio appears to be that of the gelatin-cellulose of 75÷25. Indeed, increasing the gelatin content could improve the quality and behaviour of the membrane.

The SEM was used to observe the change in the morphological structure of the Gelatin-Cellulose Hydrogel Membrane (GCHM), the SEM image of GCHM modified with EDTA was presented in Figures 5A, 5B, and 5C. The images were taken by applying 4 kV voltage with different magnification times for the clarification of the surface. The SEM images of GCHM powder before adsorption were studied in Figure 5.

Porosity characterization is based on the presence of open pores which are related to properties such as permeability and surface area of the porous structure. The SEM image indicates the presence of bigger particles with irregular shapes (Figs. 5A and 5B). Figure 5C shows the cavities of different shapes and sizes, and larger pores between the particles could be observed which will be helpful for the solution permeating through the GCHM (Wang et al., 2018).

The high porosity provides a favourable adsorption of copper and cobalt ions (Hossan et al., 2014). The presence of such granules increases the surface area of the composite which is suitable for effective adsorption of metal ions. A visible change in surface morphology can be observed following adsorption. Small openings and holes on the surface increase the contact of the adsorption and therefore lead to pore diffusion during the adsorption process (Kabuba and Banza, 2020). A morphology that changes as the gelatin concentration increases (Fig. 5C > Fig. 5B > Fig. 5A) and consequently, several pores have been observed.

Effect of pH

While adsorption process, the surface charge of the adsorbent can change according to the acidic or alkali medium of solution pH. Figure 6 indicates that the adsorption of copper and cobalt ions has been sensibly affected by the values of pH. It has been observed that the removal efficiency was low for the pH values from 0 to 4 and increase for the pH > 4.
Kumaruzaman et al., (2017) and El-Sheikh et al., (2012) has shown that the pH in the range of 3 – 5 (acidic medium), there is a strong activity of protons (H^+) that compete with the metal ions at the functional groups onto GCHM and also the electrostatic repulsion between Cu (II) and Co (II) in solution. The maximum removal percentage of Cu (II) and Co (II) was obtained at pH 5 and 7 for copper and cobalt ions, respectively; therefore pH 5 and 7 have been selected for all the experiments in this study.

Effect of Gelatin-CNCs ratios

The effect of gelatin and CNCs ratios have played a big role on the percentage removal of both ion metals at different values of pHs. Figure 7 shows the effect of gelatin and CNCs ratio on the removal of Cu (II) and Co (II).

The result in Figure 7 shows that the percentage removal of both ion metals increased with increased of gelatin amount. The high percentage removal was 70.5 and 72.5% for Cu (II) and Co (II) at pH 5 and 7, respectively for the ratio of 3÷1. Swelling of hydrogel has been observed by Yin & Amin (2014) for pH ≥ 7 (Kamaruzaman et al., 2017). It is attributed to the presence of loan pairs from amino acid of gelatin. The electrical charge of hydrogel at pH 5 is almost equal to zero because of isoelectric point of gelatin (pI= 4.9) due to amino-acid function that does not facilitate the GCHM's swelling. Above the isoelectric point, the network is negatively charged forming anionic gel. This situation can explain why the percentage removals of copper and cobalt metals ions is low and almost closer to pH 5 (Fig. 7A).

Effect of contact time

Figure 8 represents the effect the effect of time on the percentage removal of copper and cobalt ions. Adsorption process occurred by using a thermo-shaker at the range time of 15 – 120 minutes; 0.25 g of GCHM for 100 mL of wastewater for an initial concentration of 100 mg/L. It has been reported by Liu et al. (2015) that the percentage removal was function of contact time.

The percentage removal of Cu (II) and Co (II) ions was low at time t= 0 min and progressively increase until equilibrium (t = 120 min) that means, there is many available activated sites on the surface of GCHM that can adsorb copper and cobalt ions (Hossan et al., 2014). Compared with the adsorptions of Cu (II) and Co (II) to other adsorbents (Al-Shahrani, 2014; Hossan et al., 2014), the sorption equilibrium has not been reached quickly. This can be due to the low adsorption capacity of GCHM or can be attributed also to high initial concentration of Cu (II) and Co (II) and the mass adsorbent (0.25 g/100 mL).

Effect of temperature

It has been observed in Figure 9 that the negative effect of the temperature on the adsorption of Cu (II) and Co (II) onto GCHM. The percentage removal decreases while the temperature increases from 30°C – 70°C.

The percentage removal of Cu (II) and Co (II) was decreased from 70.5 to 30.8% and from 63.8 to 24.1% at pH 5 for Cu (II) and Co (II), respectively. At pH 7, the percentage removal decreases from 69.1 to 27% and from 74.5 to 32.2% for Cu (II) and Co (II), respectively. The adsorption process was an endothermic process because the removal capacity decreases while the temperature increases and this means that the available activated site onto GCHM decrease (Reshtnyak et al., 2012). It was observed the disintegration of GCHM while temperature was

gradually increased, and the filtration become difficult after adsorption process. This is the reason why is better to work with the less temperature. Therefore, the temperature of 30°C was chosen to run all the experiments.

Adsorption isotherms

Adsorption equilibrium data of Cu (II) and Co (II) – GCHM system have been investigated using three different isotherm models.

Langmuir isotherm (see Eqs. 3 and 4)

$$\frac{Ce}{qe} = \frac{1}{qm\ KL} + \frac{Ce}{qm} \quad (3)$$

$$RL = \frac{1}{1+KL\ Co} \quad (4)$$

where C_e is equilibrium metal concentration; q_m is the adsorption maximum capacity (mg/g), K_L Langmuir constant (L/ mg), q_e is the amount of metal ion adsorbed at equilibrium and R_L is a constant of separation (Mobashespour et al., 2014; Blahovec and Yanniotic, 2009).

Freundlich isotherm (Eq. 4)

$$\ln qe = \ln Kf + \frac{1}{n}\ln Ce \quad (5)$$

where C_e is the amount of metal at equilibrium (mg/L); q_e: amount of metal adsorbed at per unit mass at equilibrium (mg/g), n: Freundlich constant describing the affinity of metal for the adsorbent and K_f: Freundlich constant.

Dubinin-Radushkevich isotherm (see Eqs. 6, 7 and 8)

$$\ln qe = \ln q_m - \beta\psi^2 \quad (6)$$

$$\psi = RT \ln (1+1/C_e) \quad (7)$$

$$E = \frac{1}{\sqrt{2\beta}} \quad (8)$$

where q_m (mg/g): metal maximum adsorption capacity, ψ: Polanyi potential and β (mol^2/J^2): coefficient related to free energy of adsorption, E (kJ/mol): energy, R: universal gas constant (8.314 $mol^{-1}K^{-1}$).

The best fit for an isotherm is giving by an R^2 closest to 1. The adsorption isotherms for Cu (II) and Co (II) were studied using ratio 3÷1 for a mass of 0.25 g at 303 K. The data obtained from linear Langmuir, Freundlich and D-R isotherms plot from the adsorption of Cu (II) and Co (II) onto GCHM are presented in Table 3.

The results reported in Table 3 indicate that Cu (II) and Co (II) fit the experimental data for the Freundlich isotherm model. The monolayer adsorption capacities of hydrogel for Cu (II) and Co (II) are 5.85 and 10.99 mg/g, respectively. Cu (II) and Co (II) shows a good affinity and have been favourable to be adsorbed by hydrogel because $1 < n > 10$. The Freundlich constant were 0.83 and 1.31, respectively for Cu (II) and Co (II) (Akpomie et al., 2015). Adsorption process has been favourable to the Langmuir model because the R_L value was 0.23 and 0.16 for both metal ions (Garcia-Diaz et al., 2018).

Kinetic studies

The kinetic parameters for the adsorption process were studied on the batch adsorption at pH 5 and 7 at 303 K.

Pseudo first order model (see Eq. 9)

$$\log (q_e - q_t) = \log q_e - (k_1 t/2.303) \quad (9)$$

Pseudo second order model (see Eq. 10)

$$1/q_t = (1/k_2 qe^2)t + (1/q_e) \quad (10)$$

where q_e: amount of metal at adsorbed at equilibrium, q_t: amount metal adsorbed at a *t* time (mg/g) and k_1 and k_2: rate constant of the reaction (min^{-1}) for first and second order, respectively (Fosso-Kankeu, 2018).

From the values of R^2 represented in Table 4, it was observed that both metal ions are fitting the pseudo first order kinetic.

Kinetic diffusion

Kinetic diffusion mechanism has been investigated in order to determine the nature of adsorption of Cu (II) and Co (II) to the interface of GCHM. Three transport processes were investigated as film diffusion (see Eq. 11), particle diffusion (see Eq. 12) and moving boundary (see Eq. 13) (Garcia-Diaz et al., 2018).

$$\ln\left(1 - \frac{qt}{qe}\right) = -Kt \quad (11)$$

$$\ln[1 - (qt/qe)^2] = -Kt \quad (12)$$

$$3 - 3[1 - (qt/qe)]^{\frac{2}{3}} - 2\frac{qt}{qe} = Kt \quad (13)$$

where K (1/min) is the rate constant model, q_e and q_t (mg/g) are the sorption capacities at equilibrium and contact time, respectively, and *t* is time (min).

The moving boundary, particle diffusion and film diffusion model of ln (1 – F) versus time were taken for Cu (II) and Co (II) ions and presented in Table 5 at pH 5 and 7. The regression coefficient (R^2) values of 0.98 for Cu (II) and 0.91 for Co (II) have shown a good fit of film diffusion. The results obtained by kinetic diffusion show that the adsorption of both metal ions onto GCHM could be better explained by the film diffusion model where the rate constant models are 0.032/min for Cu (II) and 0.046/min for Co (II).

Thermodynamic studies

$$\Delta G° = - RT \ln K_d \quad (14)$$

K_d is equilibrium constant that can be used to determine the thermodynamic parameters (H°) enthalpy, (S°) entropy and (G°) free energy, R (8.314 J/mol K) universal gas constant and T is the temperature (K) (Sandoval-Flores et al., 2018).

$$\Delta G° = \Delta H° - T\Delta S° \quad (15)$$

$$K_d = q_e/C_e \quad (16)$$

$$-\ln K_d = (\Delta H°/R).\ 1/T – (\Delta S°/R) \quad (17)$$

The values of ΔH° and ΔS° from the slope and intercept of the $\ln K_d$ versus 1/T through the Von't Hoff line Equation's (Hino et al., 2010).

The thermodynamic parameter values are summarized in Table 6. The negative values of ΔG° obtained almost at all temperatures for both metal ions indicate that the adsorption process was spontaneous. It was also observed that the change in Δ°G increase with increase in temperature suggesting that higher temperatures is not making the adsorption easier. The positives values of ΔH° indicate an endothermic process. In physical adsorption process, the ΔH° < 40 kJ/mol.K. (Akpomie et al., 2015). The value of ΔH° obtained from both metal ions showed a physical adsorption process onto the surface of GCHM. This physical adsorption explains the reason why the kinetic data did not fit the pseudo second order (chemical sorption). In addition, the positive values of ΔH° indicated that the adsorption process of both metal ions was endothermic (Hino et al., 2010). Positive values of ΔS° indicate an increase in randomness at the solid/liquid interface during adsorption. The positive value of ΔS° indicated that the reflected the affinity of GCHM for Cu (II) and Co (II) and suggested some structural changes in GCHM.

Conclusion

The results obtained in this study prove that GCHM is a potential and useful low-cost material for the removal efficiency of Cu (II) and Co (II) ions from mining processes wastewater. Optimum removal of both heavy metal ions was obtained at ratio 3÷1 and at pH 5 and 7 for Cu (II) and Co (II), respectively and a contact time of 120 mins was utilized for equilibrium removal. Freundlich isotherm model gave the best fit to the experimental data for both metal ions. The positive values of $\Delta H°$ indicate that the process was endothermic, negative values of $\Delta G°$ showed the spontaneous nature of the process and positive values of $\Delta S°$ reflect an increase in randomness during the adsorption Cu (II) and Co (II) onto GCHM. Kinetic of adsorption of heavy metal ions onto GCHM was effectively described by pseudo first order and physical nature adsorption.

Credit Authorship contribution statement

JK analysed the conceptualization, methodology, validation, formal analysis, investigation, data curation, writing - original draft, writing - review & editing, visualization, resources.

TL performed the methodology, validation, investigation, formal analysis, data curation, writing - original draft.

Declaration of competing interest

The authors have declared no conflict of interest.

Ethical approval: Not applicable.

Consent to participate: Not applicable.

Consent to publish: Not applicable.

Funding: Not applicable.

Availability of data and material: Not applicable.

References

Abdulkareem SA, Muzenda E, Afolabi AS, Kabuba J. (2013). Treatment of Clinoptilolite as an Adsorbent for the removal of Copper ion from synthetic wastewater solution. Arab J Sci Eng. 38: 2263 – 2272. http://doi.org/10.1007/s13369-012-0505-x.

Abdulrahman Oyekanmi A, Abd Latiff AA, Daud Z, Saphira Radin Mohamed RM, Ismail N, Ab Aziz A, Rafatullah M, Hossain K, Ahmad A, Kamoldean Abiodun A. (2019). Adsorption of cadmium and lead from palm oil mil effluent using bone-composite: optimisation and isotherm studies. Int J Env Anal Chem. 99: 707-725. https://doi.org/10.1080/03067319.2019.1607318

Ahmed EM. (2015). Hydrogel: Preparation, characterization, and applications: A review, J Advance Res. 6: 105 – 112. https://doi.org/10.1016/j.jare.2013.07.006.

Akpomie KG, Dawodu FA, Adebowale KO. (2015). Mechanism on the sorption of heavy metals from binary-solution by a low cost montmorillonite and its desorption potential, Alexandria Eng J. 54: 757 – 767. https://doi.org/10.1016/j.aej.2015.03.025.

Alemdar A, Sain M. (2008). Isolation and characterization of nanofibres from agricultural residues-wheat straw and soy hulls, Bioresource Technol. 6: 1664 – 1671. doi.org/10.1016/j.biortech.2007.04.029.

Alizadehgiashi M, Khuu N, Khabibullin A, Henry A, Tebbe M. (2018). Nanocolloidal hydrogel from heavy metal scavenging. Nanotechnology. 12: 8160 – 8168. https://doi.org/10.1021/acsnano.8b03202.

Al-Shahrani SS. (2014). Treatment of wastewater contaminated with cobalt using Saudi activated bentonite. Alexandria Eng J. 53: 205 – 211. https://doi.org/10.1016/j.aej.2013.10.006.

Blahovec J, Yanniotis S. (2009). Modified classification of sorption isotherms. J Food Eng. 91: 72 – 77. https://doi.org/10.1016/j.jfoodeng.2008.08.007.

El Halah A, López-Carrasquero F, Contreras J. (2018). Applications of Hydrogels in the adsorption of metallic ions, Ciencia e Ingenieria. 39:1 – 28.

El-Sheikh R, Hefni HH, El-Farargy AF, Bekhit M, Negm NA. (2012). Adsorption Efficiency of Chemically modified Chitosan towards copper and cobalt Ions from Industrial Waste Water, Egyptian J Chem. 55 (3): 291 – 305. https://doi:10.21608/ejchem.2012.1156.

Feinsten R. (1995). Guide to spectroscopic identification of organic compound, CRC Press Boca Raton-London-New York, 124.

335 Fernandes de Almeida P, da Silva Lannes SD, Araújo Calarge F, de Brito Farias TM, Santana
336 JCC. (2012). FTIR Characterization of Gelatin from chicken Feet. J Chem Chem Eng. 6: 1029
337 – 1032.

338 Fosso-Kankeu E. (2018). Synthesized af-PFCl and GG-g-P(AN)/TEOS hydrogel composite
339 used in hybridized technique applied for AMD treatment. Phys Chem Earth, Parts A/B/C. 105:
340 170 – 176. https://doi.org/10.1016/j.pce.2018.02.015

341 Fujiyabu T, Li X, Shibayama M, Chung U, Sakai T. (2017). Permeation of water through
342 Hydrogels with controlled network structure. Macromolecules. 50: 9411 – 9416.
343 https://doi.org/10.1021.

344 Garcia-Diaz I, López FA, Alguacil FJ. (2018). Carbon Nanofibers: Anew Adsorbent for copper
345 removal from wastewater. Metals. 8: 914 – 927. https://doi.org/10.3390/met8110914.

346 Getachew BA, Kim S-R, Kim J-H. (2017). Self-healing Hydrogel pore-filled water filtration
347 Membranes. Environ Sci Technol. 51: 905 – 913. https://doi.org/10.1021/acs.est.6b04574.

348 Hino S, Ichikawa T, Kojima Y. (2010). Thermodynamic properties of metal amides determined
349 by ammonia pressure-composition isotherms. J Chem Thermodynam. 42: 140 – 143.
350 https://doi.org/10.1016/j.jct.2009.07.024.

351 Hossan MJ, Gafur MA, Kadir MR, Karim MM. (2014). Preparation and characterization of
352 gelatin-hydroxyapatite composite for bone tissue engineering. Polymer Composites. 14: 24 –
353 32. https://doi.org/10.1002/pc.23725.

354 Kabuba J. (2019). Equilibrium Ion-Exchange studies of Na^{+}/Cu^{2+} and Na^{+}/Co^{2+} on
355 Clinoptilolite in Industrial Wastewater. Eng Letters. 27: 467 – 474.

356 Kabuba J, Banza M. (2020). Modification of clinoptilolite with dialkylphosphinic acid for the
357 selective removal of cobalt (II) and nickel (II) from hydrometallurgical effluent. Can J Chem
358 Eng. https://doi: 10.1002/cjce.24005.

359 Kabuba J, Mulaba-Bafubiandi A, Battle K. (2014). Neural Network technique for modelling of
360 Cu (II) removal from aqueous solution by clinoptilolite, Arab J Sci Eng. 39: 6793 – 6803.
361 https://doi.org/10.1007/s13369-014-1277-2.

362 Kamaruzaman S, Aris NIF, Yahaya N, Hong LS, Razak MR. (2017). Removal of Cu (II) and
363 Cd (II) ions from Environmental Water Samples by using Cellulose Acetate Membrane. J
364 Environ Analytical Chem. 4: 1 – 8. https://doi: 10.4172/2380-2391.1000220.

Leite LSF, Moreina FKV, Mattoso LHC, Bras J. (2020). Electrostatic interactions regulate the physical properties of gelatin-cellulose nanocrystals nanocomposite films intended for biodegradable packaging. Food Hydrocolloids. https://doi.org/10.1016/j.foodhyd.2020.106424.

Liu P, Borrell PF, Božič M, Kokol V, Oksman K. (2015). Nanocelluloses and their phosphorylated derivatives for selective adsorption of Ag^{+}, Cu^{2+} and Fe^{3+} from industrial effluents. J. Hazard Mat. 294: 177 – 185. https://doi.org/10.1016/j.jhazmat.2015.04.001.

Joshi N, Rawat K, Bohidar HB. (2018). pH and ionic strength induced complex coacervation of Pectin and Gelatin A. Food Hydrocolloids. 74: 132–138. https://doi. org/10.1016/j.foodhyd.2017.08.011.

Marks R, Seaman J, Peresz-Calleja P, Kim J, Nerenberg R, Doudrick K. (2019). Catalytic Hydrogel Membrane reactor for aqueous contaminants. Environ Sci Technol. 53: 6492 – 6500. https://doi.org/10.1021/acs.est.9b01667.

Merina Paul Das, Suguna PR, Karpuram Prasad, Vijaylakshmi JV, Renuka M. (2017). Extraction and characterization of gelatin: a functional biopolymer. Int J Pharm Pharm Sci. 9: 9, 239. https://doi: 10.22159/ijpps.2017v9i9.17618.

Mobasherpour I, Salahi E, Ebrahimi M. (2014). Thermodynamics and kinetics of adsorption of Cu (II) from aqueous solutions onto multi-walled carbon nanotubes, J Saudi Chem Soc. 18: 792 – 801. https://doi.org/10.1016/j.jscs.2011.09.006.

Moon RJ, Martini A, Nairn J, Simonsen J, Youngblood J. (2011). Cellulose nanomaterials review: structure, properties and nanocomposites. Chem. Soc. Rev. 40: 3941–3994. https://doi.org/10.1039/C0CS00108B.

Münster L, Vicha J, Klofac J, Masar M, Kucharczyk P, Kuritka I. (2017). Stability and aging of solubilized dialdehyde cellulose. Cellulose. 24: 1 – 14. https://doi.org/10.1007/s10570-017-1314-x

Noorbakhsh-Soltani SM, Zerafat MM & Sabbaghi S. (2018). A comparative study of gelatin and starch-based nano-composite films modified by nano-cellulose and chitosan for food packaging applications. Carbohydrate Polymers, 189: 48–55. https://doi.org/10.1016/j.carbpol.2018.02.012.

394 Oyewo OA, Mutesse B, Leswifi TY, Onyango MS. (2019). Highly efficient removal of nickel
395 and cadmium from water using Sawdust-derived cellulose nanocrystals. J Environ Chem Eng.
396 7:103251. https://doi.org/10.1016/j.jece.2019.103251.

397 Perumal S, Atchudan R, Yoon DH, Joo J, Cheong IW. (2019). Spherical chitosan-gelatin
398 hydrogel particles for removal of multiple heavy metal ions from wastewater. Ind Eng Chem
399 Res. 58: 9900 – 9907. https://doi.org/10.1021/acs.iecr.9b01298.

400 Qi X, Lin L, Shen L, Li Z, Qin T, Qian Y, Wu X, Wei X, Gong Q, Shen J. (2019). Efficient
401 Decontamination of lead ions from wastewater by salecan polysaccharide-based Hydrogels.
402 Sustainable Chem Eng. 7: 11014 – 11023. https://doi.org/10.1021/acssuschemeng.9b02139.

403 Reshetnyak EA, Ivchenko NV, Nikitina NA. (2012). Photometric determination of aqueous
404 cobalt (II), nickel (II), copper (II) and iron (III) with 1-nitroso-2-naphthol-3,6-disulfonic acid
405 disodium salt in gelatin films, Central Eur J Chem. 10: 1617 – 1623.
406 https://doi.org/10.2478/s11532-012-0081-7

407 Sain M, Panthapulakkal S. (2006). Bioprocess preparation of wheat straw fibers and their
408 characterization, Ind. Crops Prod. 23:1 – 8. https://doi.org/10.1016/j.indcrop.2005.01.006.

409 Sandoval‐Flores G, Alvarado‐Reyna S, Elvir‐Padilla LG, Mendoza‐Castillo DI,
410 Reynel‐Avila H.E, Bonilla‐Petriciolet A. (2018). Kinetics, Thermodynamics, and
411 Competitive Adsorption of Heavy Metals from Water Using Orange Biomass. Water Environ
412 Res. 90 (12): 2114-2125. https://doi.org/10.2175/106143017X15131012188321.

413 Silva Filho EC, Santos Júnior LS, Fernandes Silva MM, Fonseca MG, Abreu Santana SA,
414 Airoldi C. (2013). Surface cellulose Modification with 2-Aminomethylpyrine for Copper,
415 Cobalt, Nickel and Zinc Removal from Aqueous solution, Mater Res. 16: 79 – 87.
416 https://doi.org/10.1590/S1516-14392012005000147.

417 Silvestein RM, Webster FX, Kiemle DJ, Bryce DL. (2007). Spectroscometric identification of
418 Organic Compound, 8th edition. Wiley. New York, 81 – 108.

419 Tran VV, Park D, Lee Y-C. (2018). Hydrogel applications for adsorption of contaminants in
420 water and wastewater treatment. Environ Sci Pollution Res. 25: 24569 – 24599.
421 https://doi.org/10.1007/s11356-018-2605-y.

422 Wang X, Liu P, Liu F, Wang X, Ji M, Song L. (2018). Adsorption Pb (II) by a polyvinylidene
423 fluoride membrane bearing chelating poly(amino phosphoric acid) and poly(amino carboxylic

424 acid) groups, Adsorption Sci Technol. 36: 1571 – 1594.
425 https://doi.org/10.1177/0263617418795531.

426 Yao Y, Wang H, Wang R, Chai Y, Ji W. (2019). Fabrication and performance characterization
427 of the membrane from self-dispersed gelation-coupled cellulose microgels, Cellulose, 26, 3255
428 – 3269.

429 Yin OS, Amin MCIM. (2014). Synthesis of chemical cross-linked gelatin hydrogel reinforced
430 with cellulose nanocrystals (CNC), AIP Conference Proceedings, 1614, 375-380.
431 https://doi.org/10.1063/1.4895226.

432 Zhang C, Li H, Yu Q, Jia L, Wan LY. (2019). Poly (aspartic acid) Electrospunnanofiber
433 Hydrogel Membrane-based reusable colorometric sensor for Cu (II) and Fe (II) detection.
434 Omega. 4: 14633 – 14639. https://doi.org/10.1021/acsomega.9b02109.

435

436

437 **Tables**

438 **Table 1.** Characteristics of the mining plant effluent used.

Parameter	Lower limit	Average	Upper limit
CODs (mg/L)	48.0 ± 0.5	50.0 ± 0.5	59 ± 1.5
NH_4^+ (mg-N/L)	36.0 ± 0.5	40.0 ± 1.5	42 ± 0.2
NO_2^- (mg-N/L)	0.90 ± 0.02	0.92 ± 0.02	0.94 ± 0.02
NO_3^- (mg-N/L)	4.0 ± 0.4	6.0 ± 0.4	10 ± 0.4
Total inorganic nitrogen (mg-N/L)	40.8 ± 0.2	45.8 ± 0.2	54.9 ± 0.2
Total Phosphorus (mg/L)	7.8 ± 0.2	9.0 ± 0.2	12.0 ± 0.2
pH	7.0 ± 0.2	7.2 ± 0.2	7.4 ± 0.2

439

440 **Table 2.** Composition of GCHM Hydrogel

	Ratio 1÷3 (%), **A**	Ratio 1÷1 (%), **B**	Ratio 3÷1 (%), **C**	Water (ml)
Gelatin	25	50	75	N/A
CNCs	75	50	25	50

441

442

443

444 **Table 3.** Calculate values of isotherm parameters, T = 303K, Ratio 3÷1, Cu $(II)_{pH5}$ and Co
445 $(II)_{pH7}$

Metal ions	Langmuir				D-R			Freundlich		
	K_L	R_L	q_m	R^2	E	q_m	R^2	n	K_f	R^2
Copper (II)	0.03	0.23	5.85	0.88	5.49	10.26	0.68	0.83	1.89×10^3	**0.89**
Cobalt (II)	0.05	0.16	10.99	0.87	7.91	15.34	0.79	1.31	3.7×10^2	**0.94**

446

447 **Table 4.** Kinetic parameters for Cu $(II)_{pH5}$ and Co $(II)_{pH7}$ adsorption onto GCHM (ratio: 3÷1),
448 concentration: 100 mg/L, dosage: 0.25 g/ 100 mL, temperature 30°C.

	First order		
	q_e	**k_1**	**R^2**
Copper (II)	25.40	3.22×10^{-6}	**0.98**
Cobalt (II)	43.45	3.81×10^{-4}	**0.91**
	Second order		
	q_e	**k_2**	**R^2**
Copper (II)	27.86	2.53×10^{-6}	0.97
Cobalt (II)	38.46	9.93×10^{-4}	0.86

449

450 **Table 5.** Adsorption mechanism kinetic parameters for Cu $(II)_{pH5}$ and Co $(II)_{pH7}$ adsorption
451 onto GCHM

	Kinetic diffusion model-Equation	**Constant**	**R^2**
Copper (II)	Moving boundary	0.017	0.86
	Particle diffusion	0.021	0.95
	Film diffusion	0.032	**0.98**
Cobalt (II)	Moving boundary	0.017	0.85
	Particle diffusion	0.035	0.89
	Film diffusion	0.046	**0.91**

452

453 **Table 6.** Thermodynamic parameters values for Cu (II) and Co (II) at pH 5 and 7, respectively.

Metal	**Temperature (K)**	**K_d**	**ΔG° (kJ/mol)**	**ΔH° (kJ/mol K)**	**ΔS° (kJ/mol K)**
Cu (II)	303	1.05	-0.11	32.73	108.08
	318	1.80	-1.56		
	333	3.29	-3.29		
	348	5.62	-4.99		

Co (II)	303	0.86	0.39	34.23	111.32
	318	1.60	-1.24		
	333	2.53	-2.57		
	348	5.26	-4.81		

454

455

456

457

Figures

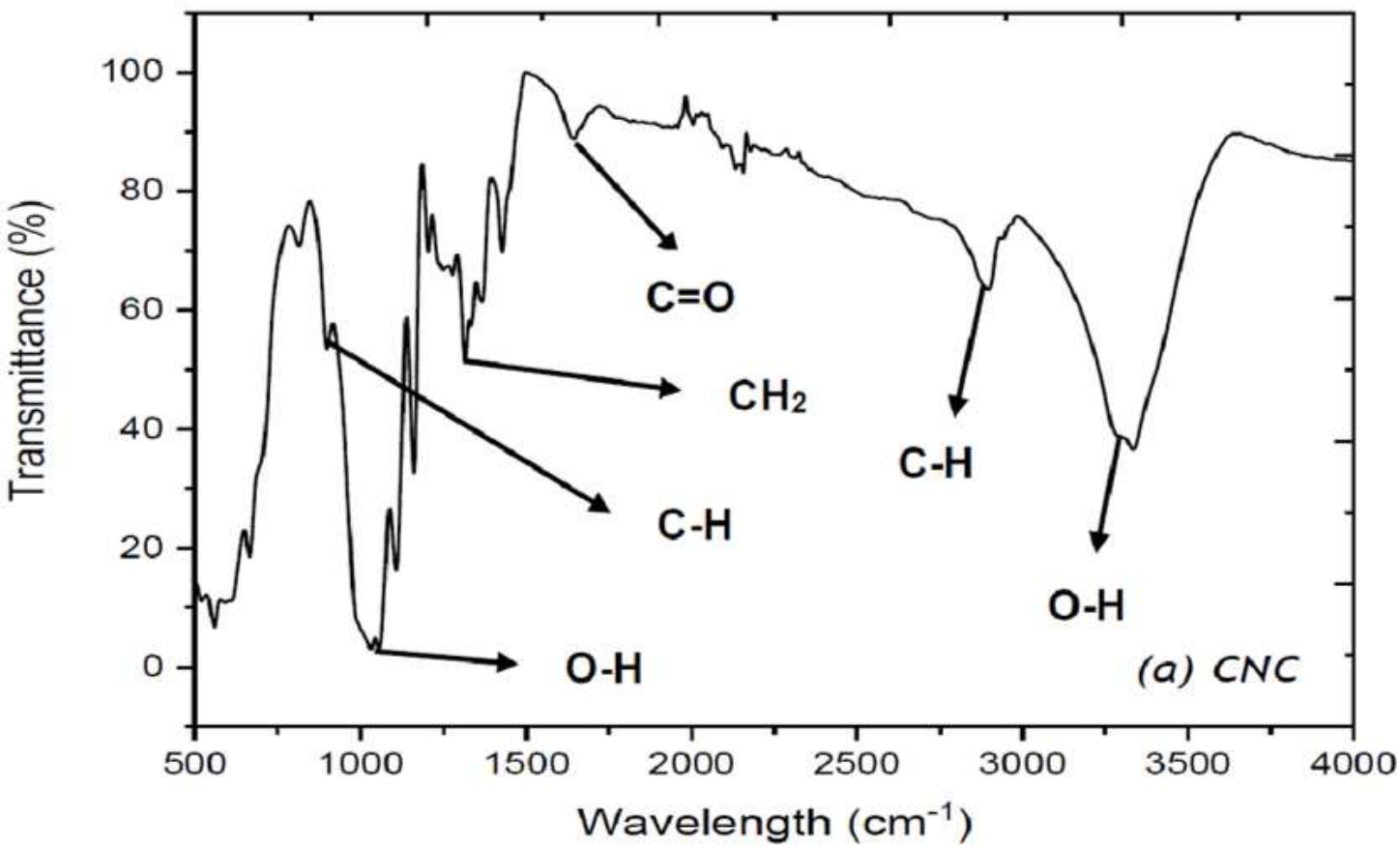

Figure 1

Spectra FTIR of CNCs

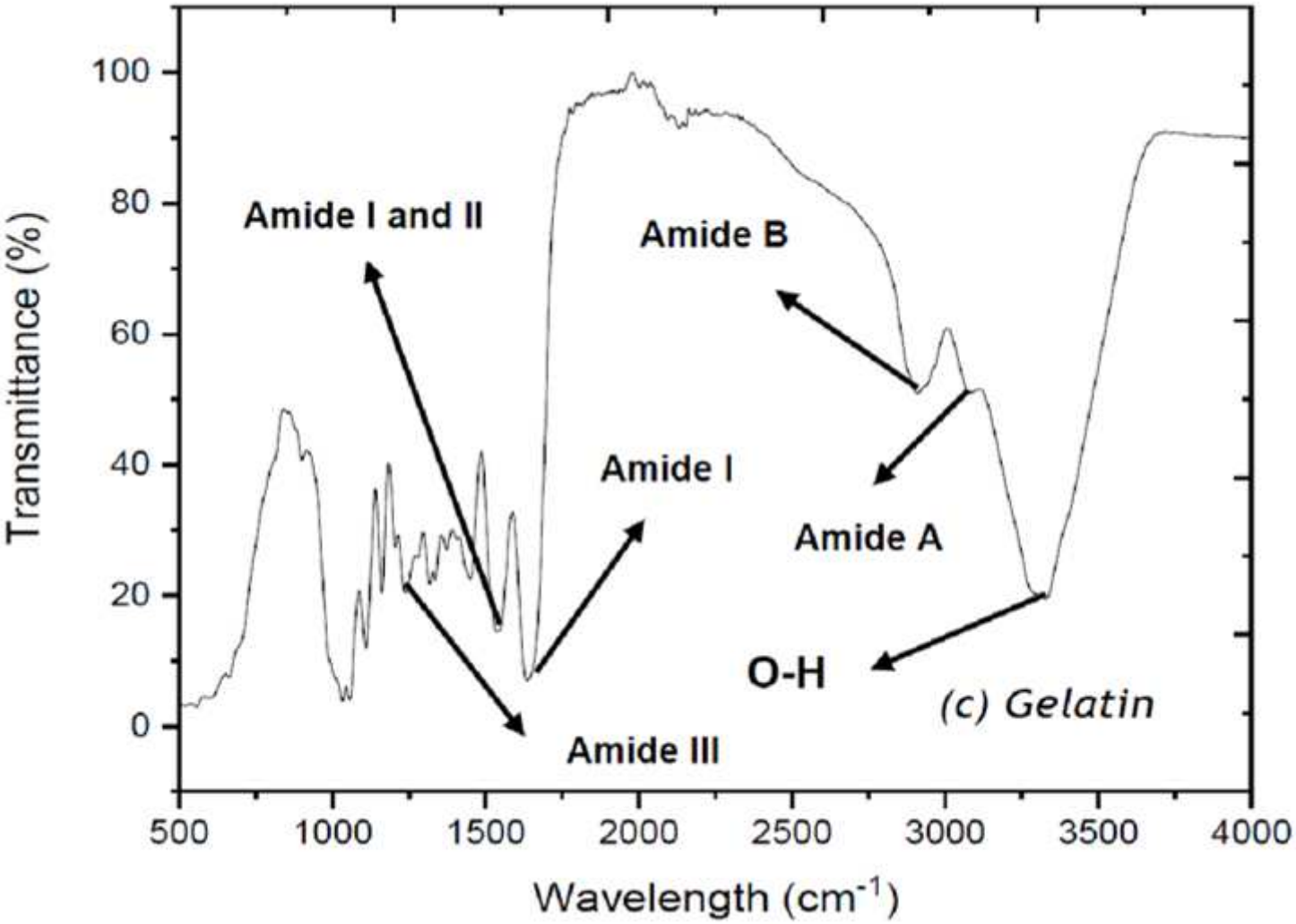

Figure 2

Spectra FTIR of gelatin

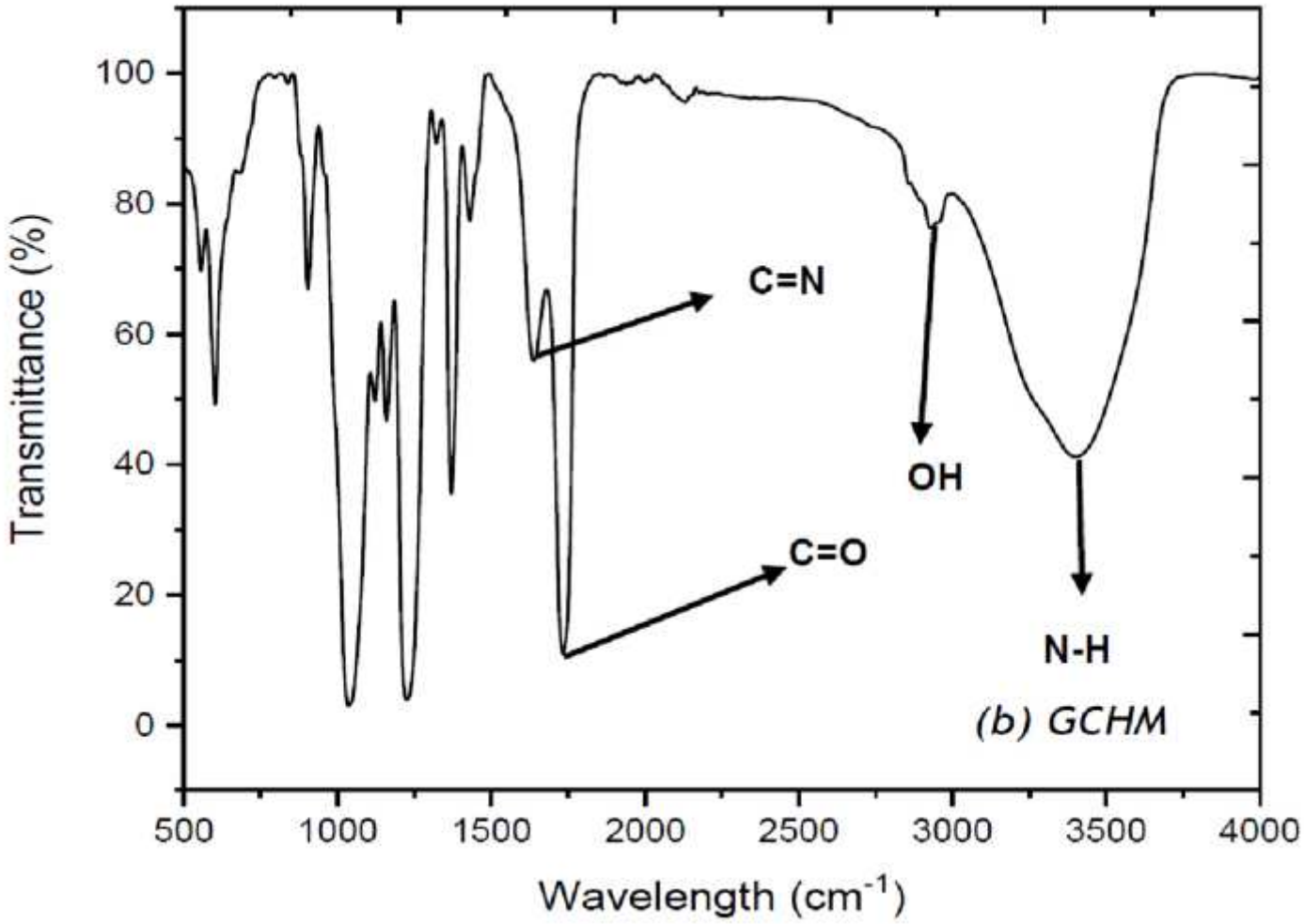

Figure 3

Spectra of Hydrogel at a ratio of 25÷75%

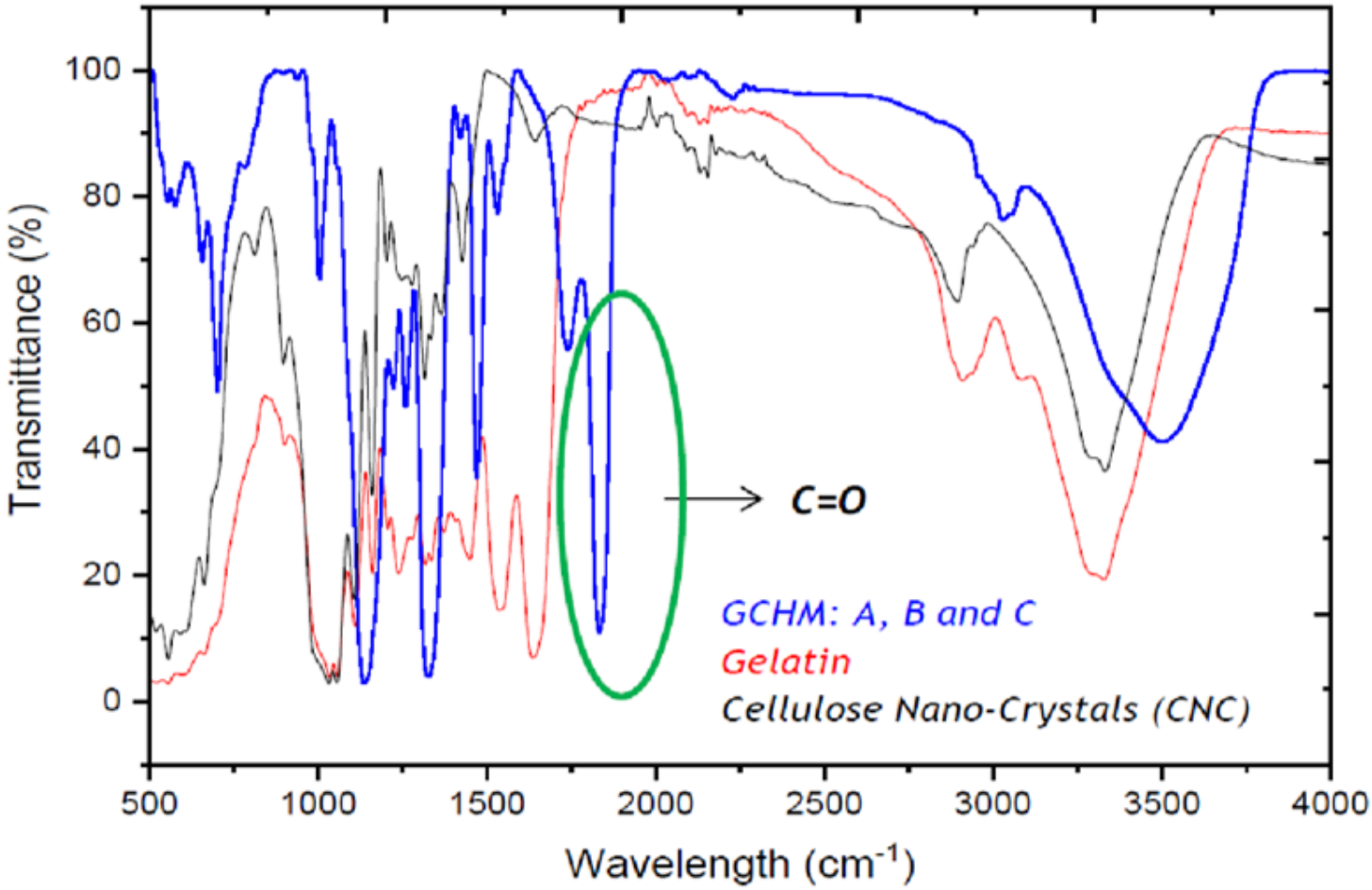

Figure 4

Spectra of CNCs, Gelatinand, GCHM

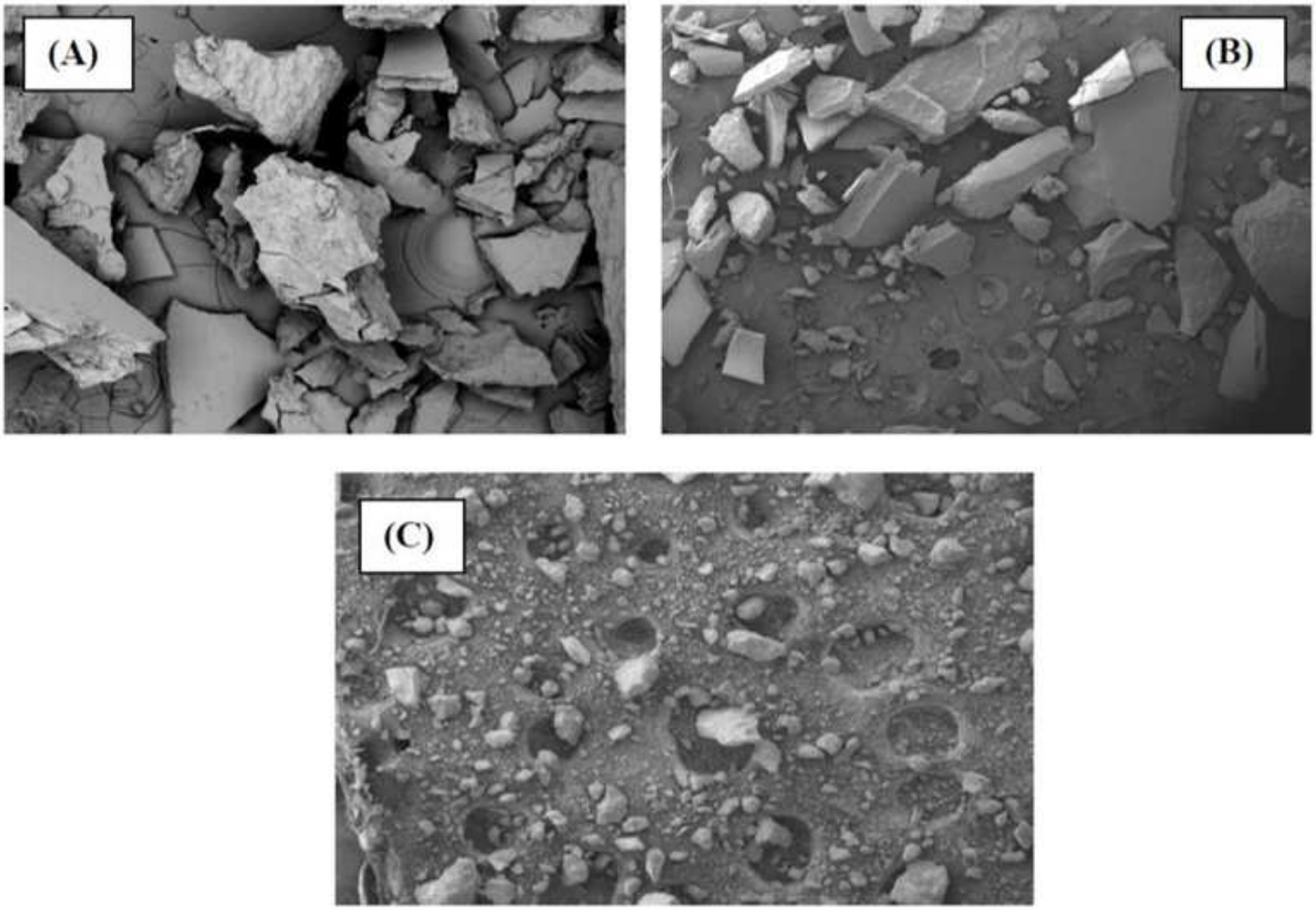

Figure 5

The SEM images of GCHM A (25÷75%), B (50÷50%), and C (75÷25%)

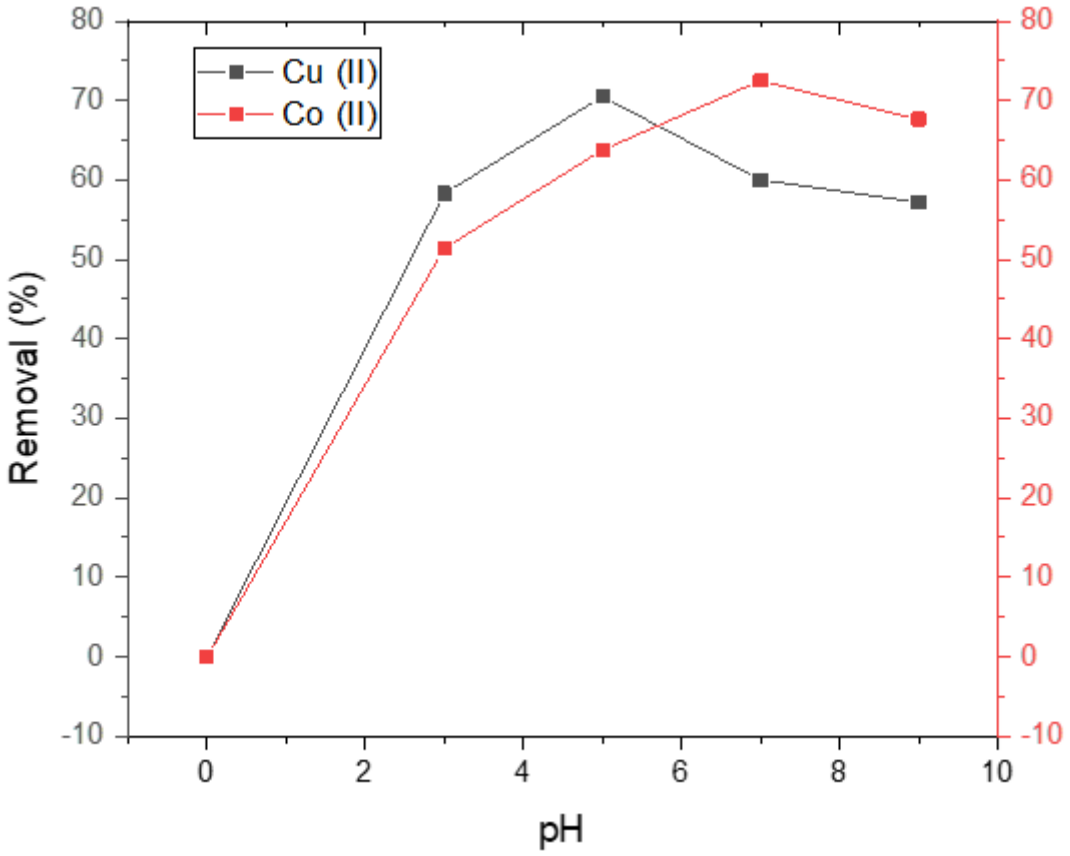

Figure 6

Effect of pH on the removal of Cu (II) and Co (II), Ratio 3÷1 at 30oC

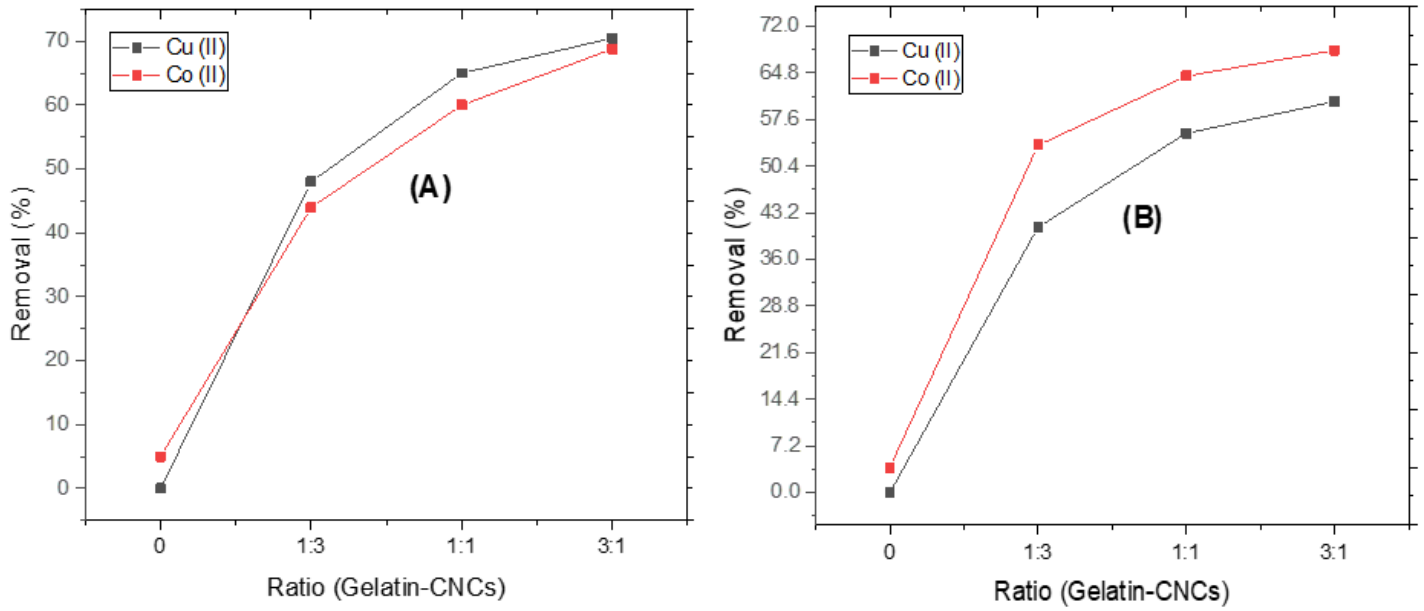

Figure 7

Effect of ratio on percentage removal of Cu (II) and Co (II), pH 5 (A) and pH 7 (B), 120 min at 30oC

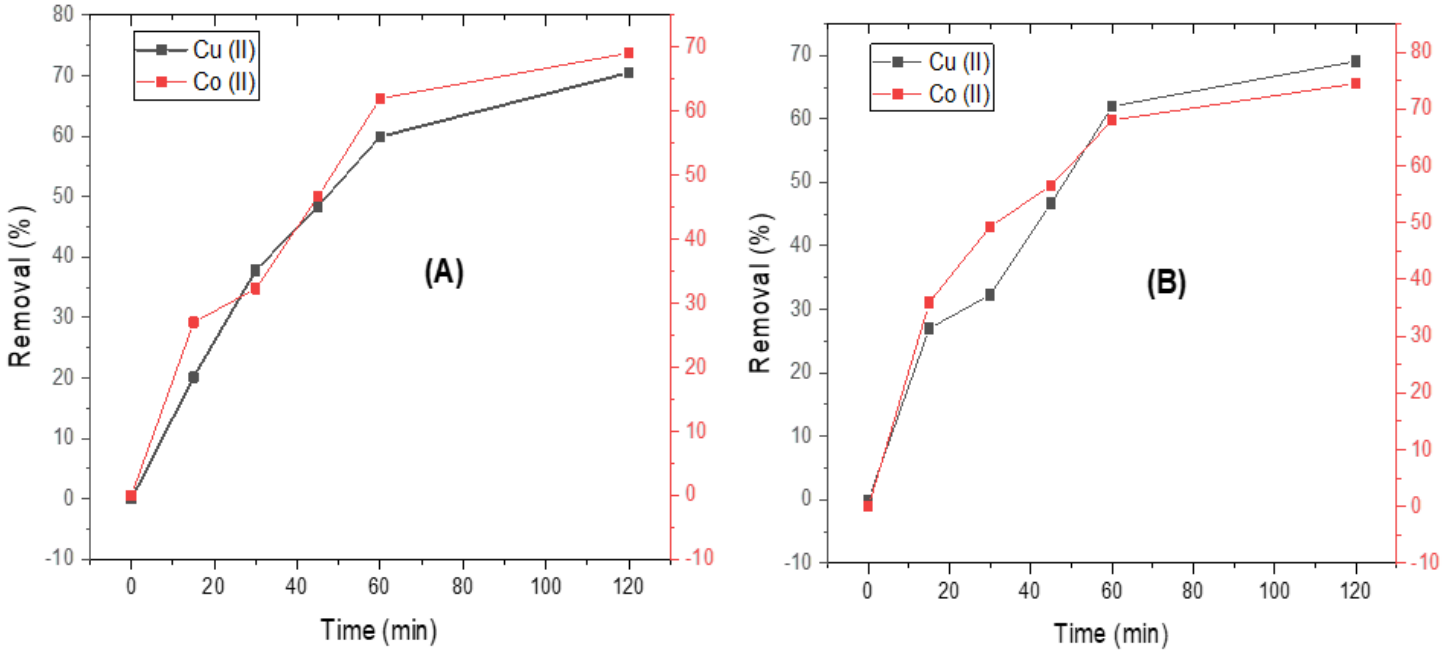

Figure 8

Effect of Time on removal of Cu(II) and Co(II), Ratio 3÷1, pH 5 (A) and pH 7 (B) at 30oC

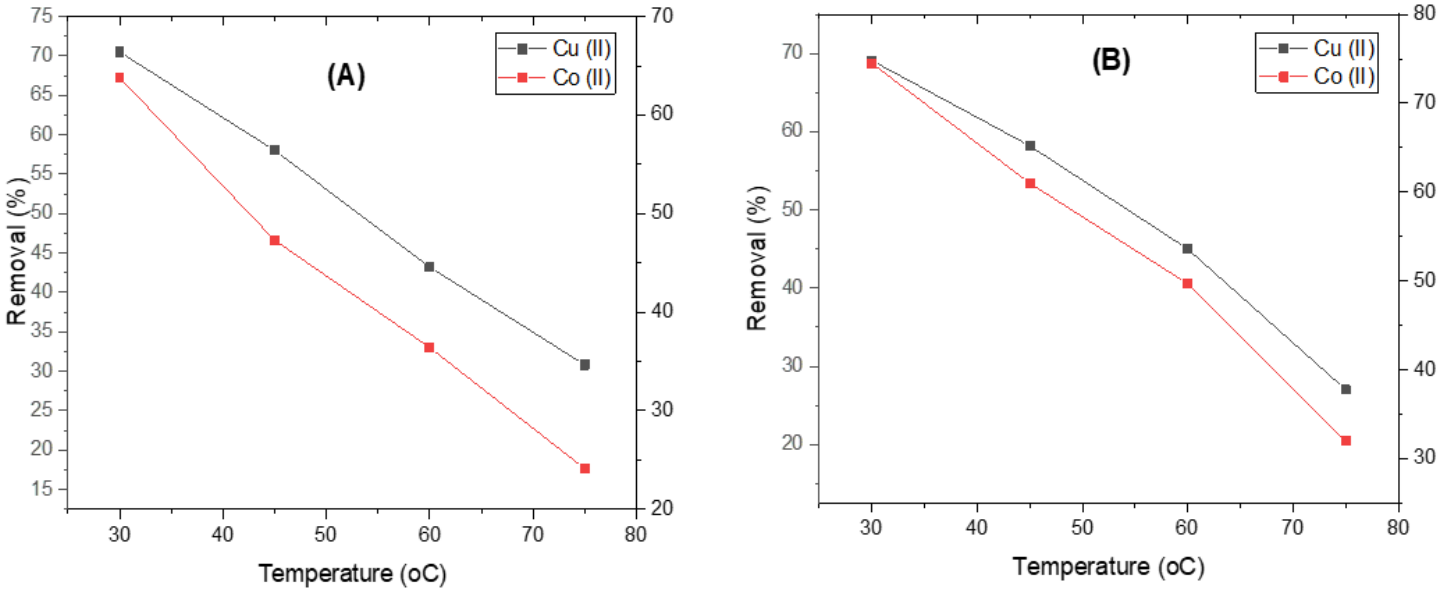

Figure 9

Effect of Temperature on the removal of Cu(II) and Co(II), Ratio 3÷1, pH 5 (A) and pH 7 (B)